AGU PUBLICATIONS

Journal of Advances in Modeling Earth Systems

RESEARCH ARTICLE
10.1002/2017MS001050

Toward a New UV Index Diagnostic in the Met Office's Forecast Model

E. C. Turner[1], J. Manners[1], C. J. Morcrette[1], J. B. O'Hagan[2], and A. R. D. Smedley[3]

[1]Met Office, Exeter, UK, [2]Centre for Radiation, Chemical and Environmental Hazards, Public Health England, Centre for Radiation, Chilton, UK, [3]Centre for Atmospheric Science, School for Earth and Environmental Sciences, University of Manchester, Manchester, UK

Key Points:
- To present a study of an improved UV Index for the UK and validate it against observations
- CAMS ozone is in general underestimated giving too high values of UV Index, more work is needed to improve vertical ozone estimates
- A hybrid ozone product using CAMS variability but monthly means gives values closer to observations

Correspondence to:
E. Turner,
emma.turner@metoffice.gov.uk

Citation:
Turner, E. C., Manners, J., Morcrette, C. J., O'Hagan, J. B., & Smedley, A. R. D. (2017). Toward a new UV Index diagnostic in the Met Office's forecast model. *Journal of Advances in Modeling Earth Systems*, *9*, 2654–2671. https://doi.org/10.1002/2017MS001050

Received 5 JUN 2017
Accepted 10 OCT 2017
Accepted article online 22 OCT 2017
Published online 19 NOV 2017

Abstract The United Kingdom sporadically experiences low ozone events in the spring which can increase UV to harmful levels and is particularly dangerous as sunburn is not expected by the public at this time of year. This study investigates the benefits to the UV Index diagnostic produced by the UM at the Met Office of including either, or both of, a more highly resolved spectrum, and forecasted ozone profiles from the ECMWF CAMS database. Two new configurations of the spectral parameters governing the radiative transfer calculation over the UV region are formulated using the correlated-k method to give surface fluxes that are within 0.1 UV Index of an accurate reference scheme. Clear-sky comparisons of modeled fluxes with ground-based spectral observations at two UK sites (Reading and Chilton) between 2011 and 2015 show that when raw CAMS ozone profiles are included noontime UV indices are always overestimated, by up to 3 UV indices at a low ozone event and up to 1.5 on a clear summer day, suggesting CAMS ozone concentrations are too low. The new spectral parameterizations reduce UV Index biases, apart from when combined with ozone profiles that are significantly underestimated. When the same biases are examined spectrally across the UV region some low biases on low ozone days are found to be the result of compensating errors in different parts of the spectrum. Aerosols are postulated to be an additional source of error if their actual concentrations are higher than those modeled.

Plain Language Summary Providing the public with accurate forecasts of the risk of increased exposure to UV allows them to take protective measures to prevent sun damage. The UK sporadically experiences low ozone events in the spring which can increase UV and is particularly dangerous as sunburn is not expected by the public at this time of year. This study investigates the benefits to the UV Index produced by the Met Office of including either, or both of, more detail in the calculation of the relevant energy at UV wavelengths, and real-time estimates of the vertical ozone distribution. A comparison of modelled UV with ground-based measurements on cloud-free days at two UK sites (Reading and Chilton) between 2011 and 2015 show that when ozone profiles are included noontime UV indices are always overestimated, by up to 3 UV indices when ozone is unusually low and up to 1.5 on a typical clear summer day, suggesting the ozone concentrations used are too low. A more detailed calculation of the UV Index can actually make the result worse due to exasperating the errors produced by the incorrect ozone. Creating a spliced ozone distribution reduces these errors to 1.5 and 1 UV indices respectively.

1. Introduction

The part of the ultraviolet (UV) spectrum between 250 and 400 nm has both beneficial and detrimental effects on human health. It simultaneously imparts vitamin D, which is vital for well-being, while carrying the risk of sunburn, DNA damage and nonmelanoma skin cancer, which varies according to an individual's dermatological makeup (Webb et al., 2016). It is a common public misconception that sun damage is based solely on temperature (Carter & Donovan, 2007). Whereas this can give an indication of risk, the dominant factors influencing UV at the surface are solar zenith angle (SZA), which is directly related to time of year and time of day, stratospheric ozone concentration, and clouds (type and distribution). SZA is predictable year to year; however, total column ozone can vary by 50% on time scales of just a few days over mid to high latitudes. Low ozone events (LOEs) are sporadically observed in the boreal spring as a result of

advection of ozone-poor polar air masses (Bronnimann & Hood, 2003; Keil et al., 2007)—a process unrelated to the photochemical destruction of ozone that leads to the Antarctic spring ozone hole. Although these events can be forecast meteorologically, the risk of sunburn is not expected by the public or outdoor workers at this time of year. Accurately forecasting UV radiation can help prevent this damage by allowing meteorological services to issue advanced warnings to the public so they can take appropriate action. However, models need to be able to predict ozone adequately and additionally represent the transfer of UV radiation through the atmosphere with sufficient accuracy. This study presents an investigation into improving the UV Index (UVI) diagnostic—the global metric commonly used to describe the likelihood of sunburn—for the forecast model operated at the Met Office, the national weather service for the UK.

The UV Index was introduced in Canada in 1992 (Wilson, 1993), to address growing concerns surrounding the damaging effects of UV radiation and its relation to ozone loss, compounded by increased exposure due to a change in peoples' leisure habits since the first half of the 1900s (Long et al., 1996). It was subsequently adopted by the World Health Organisation (WHO, 2002) and recommended as a global standard. It is defined as

$$\mathrm{UVI} = 40\,(\mathrm{m}^2/\mathrm{W}) \int_{250\,\mathrm{nm}}^{400\,\mathrm{nm}} S_\lambda E_\lambda d\lambda, \tag{1}$$

where S_λ is the spectral solar irradiance at the surface ($\mathrm{W/m^2/nm}$), and E_λ is the erythemal action spectrum (EAS), which describes the relative effect of the UV spectrum at different wavelengths at producing erythema (sunburn). UVI is a dimensionless scale and the range of global values greatly varies. The scaling factor of 40 was originally chosen to provide a range of values from 0 to 10 (10 being the highest value likely in Canada); however, Australia and New Zealand can experience values exceeding 16 (Gies et al., 2004). In the UK, 8 is rarely exceeded. A value more than 3 means sun protection is advised and beyond 6 means high risk of harm from unprotected sun exposure. The International Commission of Illumination (CIE; International Standardisation Organisation, 1998) defines the EAS as

$$\begin{aligned} E_{250 \le \lambda \le 298\,\mathrm{nm}} &= 1.0, \\ E_{298 < \lambda \le 328\,\mathrm{nm}} &= 10^{0.094(298-\lambda)}, \\ E_{328 < \lambda \le 400\,\mathrm{nm}} &= 10^{0.015(140-\lambda)}, \end{aligned} \tag{2}$$

which is shown in Figure 1 alongside the two other forms of action spectra that can harm the skin, DNA damage (Setlow, 1974) and photocarciogenic skin cancer (de Gruij, 1995). Action spectra that are beneficial to the skin: such as that producing vitamin D (Webb et al., 2011), are not shown. The shaded area is a physical interpretation of the UVI resulting from the convolution of the EAS with the surface flux for a clear summer day in southern UK. Only the erythemal response is included in the definition of the UVI; however, there are parallels with the other action spectra beyond 300 nm. The skin's erythemal response is significantly diminished at wavelengths greater than 330 nm and as almost all radiation is typically attenuated by stratospheric ozone between 250 and 290 nm most of the contribution of the index originates from between 290 and 330 nm, with a peak at 310 nm, the majority being UV-B and the longer wavelength tail being UV-A according to the classifications recommended by the CIE (ISO-21348). Figure 2 shows the same convolved UV flux (small red line) in relation to the incident UV radiation at the top of atmosphere and the Earth's surface. The main clear-sky atmospheric components that modify it are stratospheric ozone and, to a much lesser extent, oxygen absorption and Rayleigh scattering.

Models that calculate UV Index tend to fall into three categories, with decreasing complexity. These are multiple scattering models, fast models and empirical models. Koepke et al. (1998) provides a comparison of 18 UV Index models of the various types. The first type of model contains a full radiative transfer calculation for an input atmospheric vertical profile, including a treatment of scattering at each model level. The second type applies a faster analytical function to the atmospheric profile that has been derived from more precise radiative transfer calculations on a training set of profiles. The third is typically a relationship between dominant variables such as solar zenith angle and ozone concentration and the UV Index, which is fitted from observations, e.g., Burrows (1997) and Allaart et al. (2004). An example in the first category is the UV processor developed by the European Centre for Medium-Range Weather Forecasts (ECMWF), that takes 3-D fields from the Integrated Forecast System (IFS) model and calculates fluxes using the Delta-Eddington method in the range 280–440 nm at either 5, 1, or 0.5 nm resolution (Morcrette & Arola, 2007). At these resolutions a

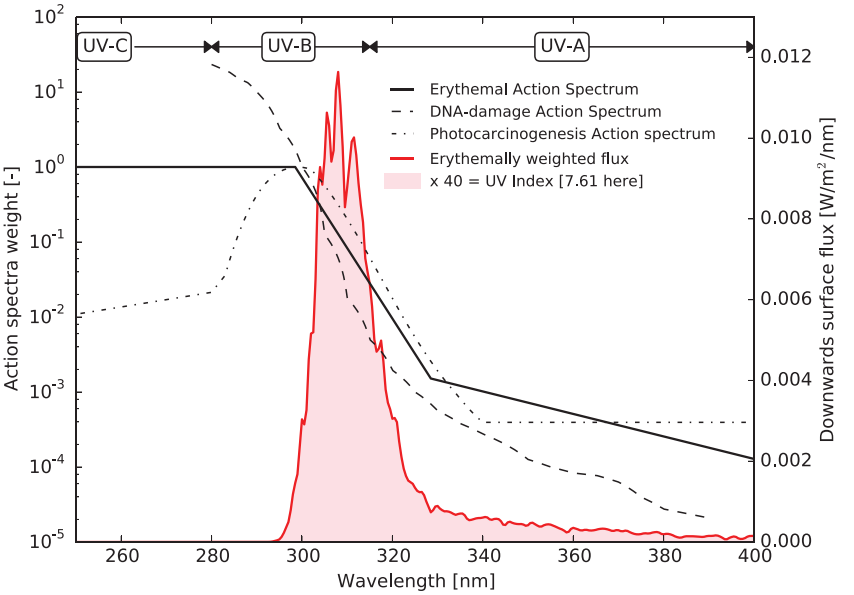

Figure 1. An example of the erythemally weighted spectral flux at the surface (red line) and various action spectra relating to sun damage. UV Index is the integral of the convolved flux scaled by 40 (equation (1)) which is represented by the region shaded pink. The fluxes are calculated from clear-sky atmospheric profiles in the southern UK for 12:00 UTC on 23 June 2015. The subdivision of the spectrum into the UV-A, UV-B, and UV-C classifications recommended by the International Commission of Illumination (CIE) are labeled at the top.

minimum of either 24, 120, or 240 calculations are made per value of UV Index, one for each spectral point. In order to reduce computational costs when run hourly within the IFS cycle, only those model grids where the cosine of the solar zenith angle is higher than 0.01 are retained. For hourly operational use as part of a high spatial resolution numerical weather prediction model such as the Met Office's regional UK model

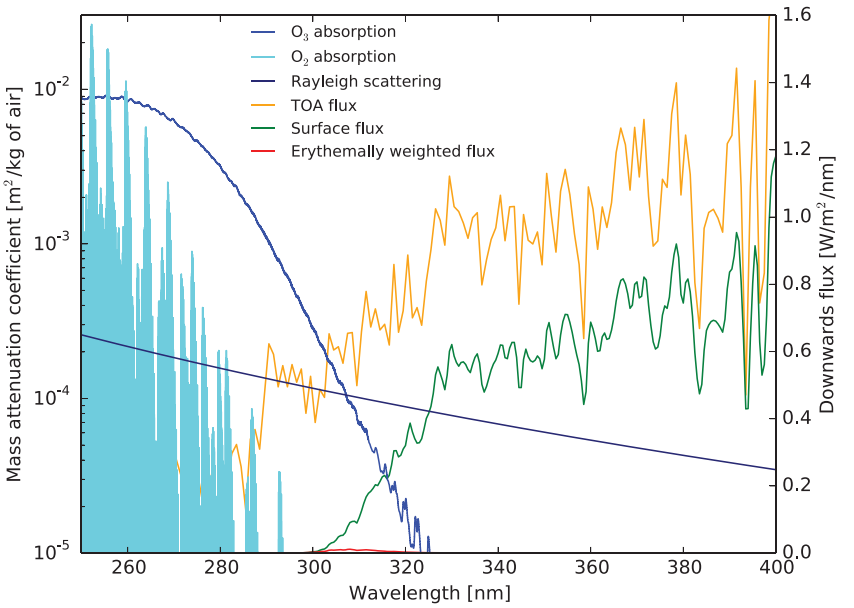

Figure 2. The solar spectrum in the UV region at the top of atmosphere and the Earth's surface (right ordinate axis) and the primary attenuators of radiation: ozone and oxygen absorption and Rayleigh scattering (left ordinate axis). The spectrum of top of atmosphere flux is an average of satellite measurements made over the period 2000–2011 (Lean & DeLand, 2012). The surface spectra for clear skies is calculated using the radiative transfer method described in section 2.1.2. The same EAS weighted surface flux presented in Figure 1 is shown for scale.

(Clark et al., 2016), which currently has a ~1.5 km horizontal grid length, this computation is still too expensive.

In the Met Office Unified Model, the cost of the radiative transfer calculations is reduced by using the correlated-k method (Goody et al., 1989), where for each band of wavelengths and gaseous species, line-by-line absorption coefficients are reordered by ascending magnitude and replaced by a smaller subset of these coefficients with associated weights to approximate the results given by the full set. The weights remain the same for each layer while the coefficients are correlated and scaled by layer values of pressure and temperature. There is no unique method for identifying the optimum number of correlated k-terms or placement of bands for a particular purpose as each spectral region has different features (Zhong & Haigh, 2000). For a single band, the method of Cusack et al. (1999) seeks to retain as few k-terms as possible while conserving the transmission function in each interval which is reasonably good for GCMs. However, as discussed in section 3, there are multiple other factors to consider in the UV region in order to determine the best configuration.

It is a strict test for UV models to reproduce observed values. Previous studies have used ground-based and satellite-derived measurements to deduce biases in models and observing systems, and create past climatologies of UV quantities (e.g., Kazantzidis et al., 2015, and references therein). In this study, ground-based spectral observations of erythemally weighted UV indices are compared with their modeled counterparts over the diurnal cycle on days between 2011 and 2015 that are identified as completely clear. This tests the chosen correlated-k spectral parameterization, and the ingested atmospheric state, particularly how the vertical ozone distribution is represented. If the model reproduces past observations well this gives us confidence in its ability to forecast future UV indices. It should be noted that, given the considerable uncertainties associated with modeling clouds and their radiative effects, this study only considers the clear-sky challenges in calculating UV Index. Fortunately this is the most relevant quantity to impact human health.

The rest of the paper is organized as follows: the radiative transfer model used by the Met Office, ozone measurements and the sources of observational UV data are discussed in section 2, the selection of spectral characteristics for calculating the UV Index is described in section 3, a comparison of simulated indices and ground-based observations for selected low ozone and/or clear days at two UK sites is presented in section 4, and recommendations for future work are given in section 5.

2. Data and Methods

2.1. SOCRATES and the Unified Model

The Met Office is unusual amongst national meteorological centers in that a single atmospheric model is used across all time and spatial scales, so both regional weather forecasts and long-term global climate projections use the same underlying physics and dynamical equations, hence the name Unified Model (Brown et al., 2012). Incremental updates to the operational global atmospheric (GA) configuration are periodically frozen and numbered, such as GA 7.0. The radiative transfer model used in the GA series of models is the Suite Of Community RAdiative Transfer codes based on Edwards and Slingo (SOCRATES; https://code.metoffice.gov.uk/trac/socrates; Edwards & Slingo, 1996). The code is flexible in that all characteristics pertaining to the spectrum are specified in a separate "spectral file." For GA7 gaseous absorption is treated by using the correlated-k method with six solar bands and nine thermal bands.

Full radiation calculations are performed hourly using a mean solar zenith angle for the proceeding hour, and corrections to the fluxes are made based on the cosine of the instantaneous solar zenith angle, at intervening model time steps (such as every 10 min) as described by Manners et al. (2009). For a more detailed description of the radiation scheme, including the treatment of clouds and aerosols, see Walters et al. (2017, section 2.3).

2.1.1. UM UV Index

The existing UV Index in the UM is forecast up to five days into the future using an empirical parameterization applied to the downward surface flux produced by the first band of the broadband shortwave scheme. This band covers 200–320 nm and uses six absorption coefficients for ozone and one Rayleigh scattering coefficient. A multiplicative factor of 3.6 is applied to the total flux in this band to give a good approximation of the UVI calculated with the convolved EAS given by equation (1) to give

$$\mathrm{UVI_{UM}} = 3.6\,\mathrm{m^2/W} \times S_{200-320\,\mathrm{nm}}. \quad (3)$$

This is referenced as the one band spectral file in the text.

2.1.2. Model Profiles for SOCRATES Offline Calculations

A key advantage of the SOCRATES formulation is that it can be run offline using custom input profiles as a stand-alone radiative transfer model. This provides the flexibility to use an instantaneous solar zenith angle to correspond with observations, and also to apply a variable ozone profile, as opposed to the current monthly and zonally meaned climatology implemented in the UM (see section 2.2). Having identified clear-sky days, atmospheric model runs are performed to obtain the vertical profiles of the atmospheric state at the grid point nearest to the observational site at hourly intervals. These thermodynamic profiles are used as the basic inputs to the offline SOCRATES calculation. The runs are performed at an N320 L70 configuration which corresponds to approximately 25 km horizontal resolution and 70 levels in the vertical extending up to 80 km. They are initialized using ECMWF analyses on 137 hybrid-pressure levels at 06:00 UTC and 12:00 UTC on the day in question. The T + 1 to T + 5 output from runs initialized at 06:00 and 12:00 UTC are calculated to produce profiles for each day of interest.

2.2. Ozone

A vertical profile of ozone is required for accurate radiative transfer modeling as UV absorption by ozone is dependent on air temperature, which is vertically variable (Forster, 1995). The current atmospheric configuration of the UM (GA7.0) uses the same zonal mean ozone climatology as its predecessors which was added in GA4.0, and is derived from the World Climate Research Programmes (WCRP) Stratospheric Processes and their Role in Climate project (SPARC-II) data set (Cionni et al., 2011). It consists of monthly means generated from satellite and ozonesonde measurements between the years 1994 and 2005 to cover a full 11 year solar cycle. The data are originally provided on 60 pressure levels between 1,000 and 1 hPa and are converted to the 70 model levels (hybrid height) used by the UM and are the same year to year. The local ozone amounts vary with each time step according to the density of the layers. A three-dimensional forecasted ozone product is required from a modeling perspective. The Copernicus Atmosphere Monitoring Service (CAMS; http://www.copernicus.eu) managed by ECMWF produces near-real-time analyses and forecasts of global atmospheric composition from 2015 onward and additionally reanalysis data sets for previous dates. CAMS uses 4D-VAR data assimilation combining in situ and remote sensing observations with Integrated Forecast System (IFS) model output. Global three-dimensional ozone fields are produced on 60 hybrid-pressure levels up to 60 km using satellite data from GOME on ERS-2, MIPAS on Envisat and MLS on Aura (see Flemming et al., 2016 for the full set of observational sources). Total column ozone is retrieved simultaneously using data from GOME-2 on MetOp-A and MetOp-B, OMI on Aura and SCIAMACHY on Envisat. CAMS ozone is available at six hourly intervals.

2.2.1. Identification of Low Ozone Events

The University of Manchester monitors ozone levels at Manchester and Reading using ground-based Brewer spectrophotometers (Smedley et al., 2012), and the Met Office operates Dobson spectrophotometers at Lerwick. If a low ozone event (LOE) is detected, Public Health England (PHE) is informed to issue appropriate public health warnings. Lower ozone is observed between November and February (in the northern hemisphere) which coincides with the highest solar zenith angles. However, large variability is common in the first half of the year as the daytime-mean solar zenith angles decreases. A LOE is officially defined as a departure of more than two standard deviations below the long-term monthly mean value for the site and a record of past LOEs meeting this criterion are shown on the UK-AIR DEFRA website (https://uk-air.defra.gov.uk/research/ozone-uv/ozone-events). Of the events listed, those additionally identified as clear-sky days over southern England were selected for analysis, resulting in a sample of five clear-sky LOE days. A fully clear diurnal cycle was determined by visual inspection of the ground-based UV measurements to isolate those with smooth bell-shaped curves. Additionally, eight clear-sky days in 2015 with typical (not low) ozone levels were analyzed in order to test the standard performance of the new diagnostic across the annual cycle.

Figure 3 shows the CAMS time series of total column ozone at Reading from 2011 to 2014 with the five LOE days indicated by a blue cross at 12:00 UTC and the corresponding total column ozone from the UM (red crosses) calculated as a sum of mean layer ozone mass mixing ratios multiplied by density and converted to Dobson units. All LOEs are below 300 Dobson Units (DU) and, with the exception of 14 January 2012, all are in the springtime (March/April). The total column ozone value on 23 April 2013 was 266 DU which is

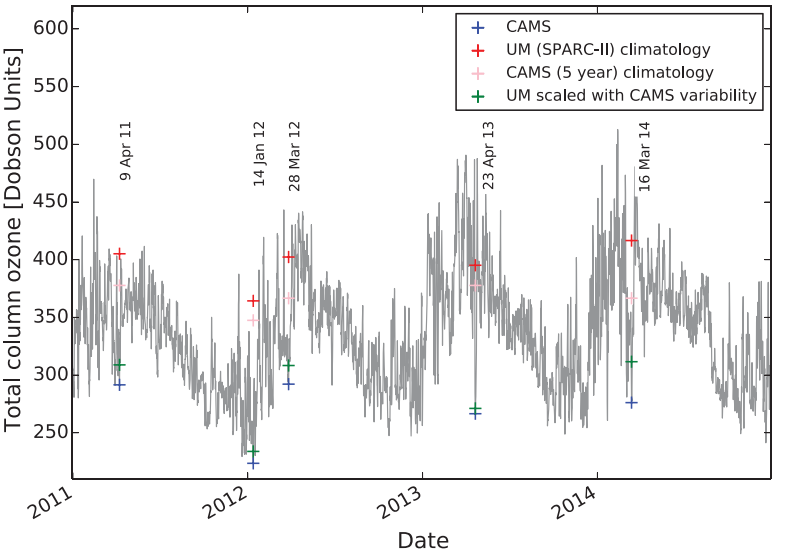

Figure 3. Total column ozone time series at Reading, UK for 2011–2014 from the CAMS analysis at 6 hourly intervals (grey line) with low ozone events indicated by crosses. Blue crosses are CAMS values at 12:00 UTC on the day in question and red crosses show the equivalent total column ozone calculated from the monthly ozone climatology used in the UM which varies over the month due to the varying vertical pressure profile. Pink crosses show the monthly mean total ozone from 5 years of CAMS data (2011–2015) and green crosses are the UM values plus the difference between the 12:00 CAMS value and the CAMS monthly mean (the variability).

unusually low for such a late date in spring, There is a small amount of cloud contamination on this day in the morning which completely clears by the afternoon and the day is retained in the sample due to the particularly low levels of ozone. For reference the lowest value ever recorded at Reading was 188 DU on the 27 December 2011. CAMS ozone values at LOEs are around 20–40% lower than the corresponding climatological values used by the UM. Figure 4 shows the same data for 2015 with the eight clear-sky days identified.

2.2.2. Rescaling of UM Climatologies

The zonal mean UM climatologies constructed from 11 years of SPARC-II data and implemented in GA4 were chosen to be accurate in the mean although they do not capture the magnitude of the ozone variability observed over the UK. This can be remedied by incorporating the variable part of the time series

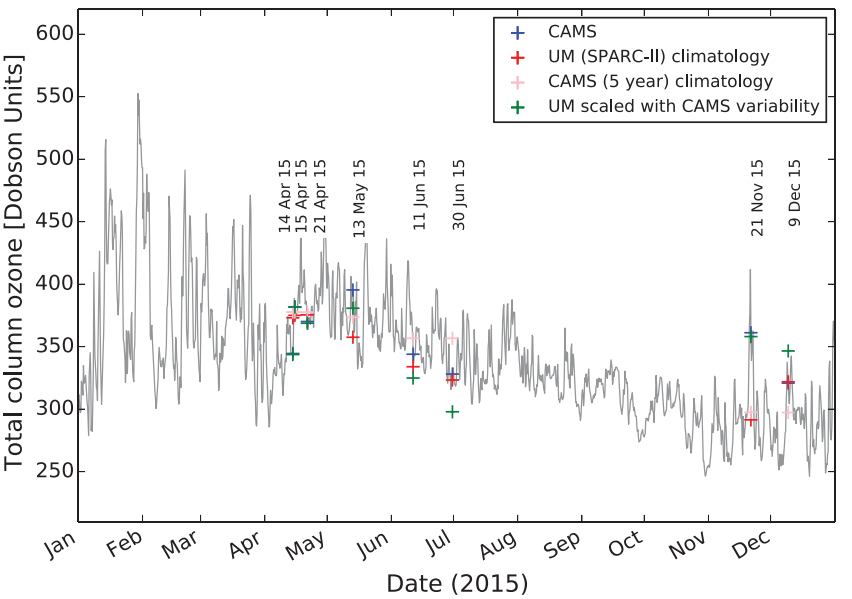

Figure 4. Same as Figure 3 but for eight clear-sky days in 2015 with typical ozone levels.

provided by the CAMS ozone prediction scheme into this mean value. This allows quantification of the benefit of capturing ozone variability without potential masking of the result from using ozone data with a different mean value. A residual is calculated between daily CAMS total ozone columns and the CAMS monthly mean value from the 5 year period between 2011 and 2015, and added to the UM total column. The change between this new value and that given by the raw UM climatology is used to scale the ozone by the same factor at all levels in the UM vertical profile. However, it should be noted that a bias could be present in the CAMS mean due to the limited 5 years used. This method of constructing the ozone profile, referred to as a "hybrid" UM-CAMS profile, is compared against the unperturbed CAMS profile and the UM climatology and all are evaluated by comparing their simulations of UVI to observations in section 4.

2.3. Empirical UV Model

In addition to the SOCRATES spectral configurations described in section 3, UV indices are calculated using the simple empirical model derived by Allaart et al. (2004) to compare results. This model only requires three inputs: total ozone column, solar zenith angle and the Sun-Earth distance. This model was created with observations from the Netherlands and Suriname via a regression equation and is judged to be valid under clear skies for all global locations, except possibly in high mountains. It does not contain any spectral information, hence, the effect of clouds or aerosols cannot be incorporated into the UV fluxes which would be needed to produce a UVI as part of an operational weather forecast model. The total column ozone value used in the calculation is from the CAMS product.

2.4. Spectral UV Observations

UV is monitored at nine sites around the UK by Public Health England using broadband detectors that measure radiation in the photopic (visible to the eye) spectral range, UVA band and total erythemally weighted UVI (https://uk-air.defra.gov.uk/data/uv-index-graphs). Additionally PHE carries out spectral UV monitoring at Chilton, Oxfordshire. The University of Manchester operates broadband and spectral detectors at Manchester and Reading. Data were obtained from these three sites in order to allow comparisons on a spectral level, but data from Manchester were discarded due to prevalent cloud contamination. The Reading instrument is a Bentham DM150 double-monochromator spectroradiometer located at the University of Reading (51.44°N, 0.94°W). The spectrum is measured every 30 min from 290 to 500 nm with a 0.5 nm sampling resolution. The Reading instrument is calibrated, and the raw spectral data is passed to the SHICrivm algorithm for homogenization (details are given by Kazantzidis et al., 2015). The Chilton instrument at the PHE site at Harwell Campus (51.58°N, 1.32°W) is a Jobin Yvon D3 180 double-monochromator spectroradiometer which records a scan every 15 min from 280 to 400 nm with a 1 nm sampling resolution. Evaluating the UVI from the model against two sets of independent observations from locations that are only 25 km apart allows any disagreement between the models and observations to be compared to observational uncertainty. As both instruments are calibrated independently, differences may arise due to a variety of factors in addition to the differing wavelength resolutions, such as the cosine response of the optical head, for example.

3. Spectral Configuration

The SOCRATES spectral file is created prior to the radiative transfer calculation by a preprocesser and contains spectrally dependent information for each band including wavelength limits, incoming solar fluxes and attenuation coefficients. The erythemal response of the spectrum is applied at this stage via an instrument spectral response, or "filter" function, which is described in Ringer et al. (2003). The erythemal weights are calculated for each wavelength band using a spline fitting technique and are used to scale the solar spectrum in the spectral file, including the modifying factor of 40 that transforms the calculated fluxes into UV indices (equation (1)). The aim in creating a new efficient spectral configuration is to minimize differences in the calculated UV indices with respect to those produced by a high-resolution reference file. The latter is constructed from 150 bands at 1 nm sampling resolution, each containing between 1 and 5 gas absorption coefficients from ozone, derived from cross sections produced by Gorshelev et al. (2014) and Serdyuchenko et al. (2014). Oxygen is found to have a negligible effect on UV Index so is not represented. Aerosols are represented by their total absorption and scattering coefficients and asymmetry as monthly climatologies produced by the CLASSIC (Coupled Large-scale Aerosol Simulator for Studies In Climate) aerosol scheme which is described in Jones et al. (2001). The UV spectral file is run alongside the existing six band

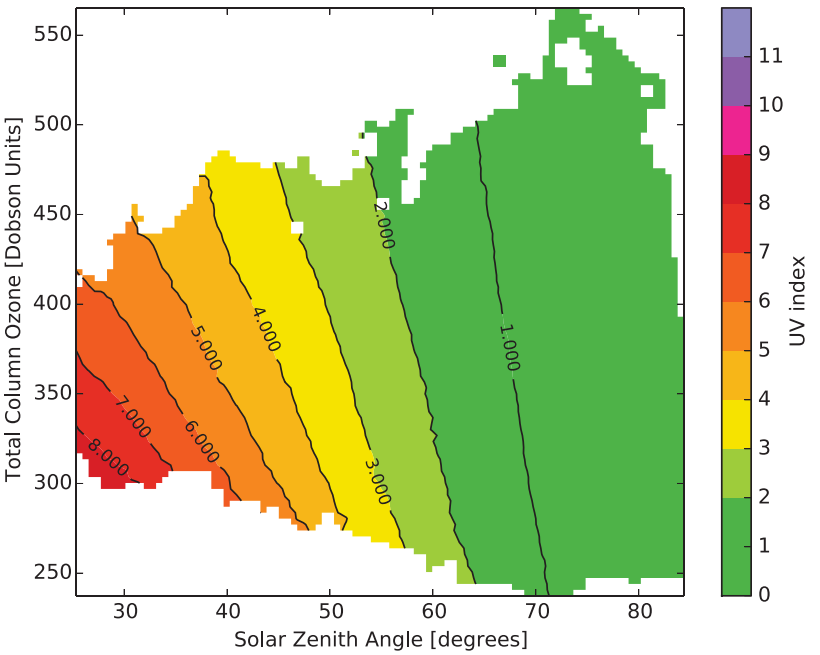

Figure 5. Mean UV Index, valid at 12:00 UTC, for the range of solar zenith angles (SZA) and total column ozone (TCO) encountered over the whole of 2015 for the UK region (9.2°W–2.0°E/48.8°N–61.2°N at 0.4° horizontal resolution) as produced by the 150 band spectral file. The average is calculated over multiple occurrences, with the data binned into 100 SZA and 100 TCO bins. The contour scale is the internationally agreed color scheme for UV Index (WHO, 2002).

shortwave spectral file in the Unified Model simultaneously; hence, the UV indices are obtained diagnostically without affecting the standard operation of the model.

Figure 5 shows the mean noontime UV indices produced with this reference file for the range of solar zenith angles and total ozone columns experienced by a grid of locations in the UK for a year of data. Determining the optimum positioning of bands for a low resolution file (each of which contains only one Rayleigh scattering coefficient) and the minimum number of ozone absorption coefficients required therein, has no analytical solution due to the number of variable factors that produce the surface values. The combined factors to consider are; the strength of ozone absorption and scattering, which decreases with increasing wavelength across the UV band (see Figure 2), their variability, which can require more absorption coefficients in a given band for large variations, and what UV flux remains as part of the UV Index at the surface, which is dependent on the spectral erythemal response as well as what has been absorbed by ozone. For example, the strength of ozone absorption at wavelengths below 290 nm is such that no flux is measured at these wavelengths at the surface, so as long as the absorption coefficients are large enough to represent this, many terms are not needed. Alternatively, this band could be omitted entirely as a good approximation. Similarly, as the skin has greatly reduced erythemal response to wavelengths above 330 nm (Figure 1) then even though more UV flux reaches the surface there is no need to model it with as great a detail as the wavelengths between 290 and 330 nm.

The dual sources of error arising from representing Rayleigh scattering with a band averaged coefficient and limiting the number of absorption coefficients within a band, can fortuitously cancel each other out by the time the flux reaches the surface. Error cancellation can be within a given band, or between multiple bands, even though biases may be large at levels above the surface. Figure 6 shows the results of this process for a 3 band spectral file with a total of 10 absorption coefficients, and for a 10 band spectral file with a total of 15 absorption coefficients. Band 2 of the 3 band file covers the 300–330 nm region and contains six absorption coefficients. The errors over the entire vertical profile are cumulatively larger than the equivalent band with more than six absorption coefficients; however, at the surface, this configuration cancels with the error produced by the band averaged scattering to bring it closer to zero for the whole range of parameter space appropriate to the UK. Using one absorption coefficient in the third band covering 330–400 nm (light blue) produces a mean negative bias that cancels closely with the positive errors in bands 1 and 2 (dark

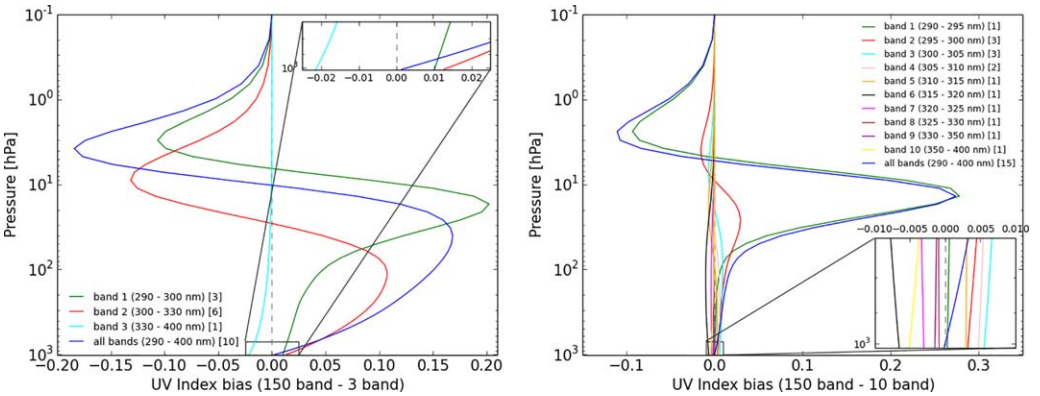

Figure 6. Band by band and total vertical biases in the UV Index for the (left) 3 band and (right) 10 band spectral files against the corresponding part of the 290–400 nm part of the 150 band file (1 nm band resolution). The bias profile is calculated at 12:00 UTC one each day of 2015 on a grid of points across the whole of the UK (32 latitudes and 29 longitudes) and the mean bias is the average over these 338,720 vertical profiles. Square brackets show the number of ozone mass absorption coefficients in each band.

blue line for the combined three bands). Increasing the number of bands at shorter wavelengths to 8 between 290 and 330 nm, bringing the total number of bands to 10, in order to reduce the Rayleigh scattering bias that has a greater effect in this region reducing errors throughout the vertical profile by at least a factor of 10 (Figure 6, right).

Figure 7 shows how the spectral files selected in this manner perform across a typical year of solar zenith angles and atmospheric ozone concentrations in the UK. Absolute values of the UVI calculated by the reference 150 band file are shown in Figure 5. The greatest biases are at low solar zenith angles and total column ozone concentrations, which is to be expected as the UVI is highest at these times. However, even for the three band configuration absolute magnitudes of the bias do not exceed 0.12 UVI. It is particularly reassuring that biases when total column ozone is less than 300 DU and solar zenith angles lie between 40° and 50° are so close to the zero contour in the 10 band file, as this is where springtime low ozone events occur.

4. UV Index Comparisons With Observations

Diurnal differences between modeled UV fluxes and observations are shown for the five low ozone events (Figure 8) and the eight ordinary clear-sky days at Chilton (Figure 9) and Reading (Figure 10). For calculations using the new spectral file configurations, only results from the three band file are shown, as differences between equivalent results from the 150 and 10 band files are so small as to be indistinguishable, with a maximum of around 0.1 (UVI). Differences between fluxes measured near simultaneously at the two

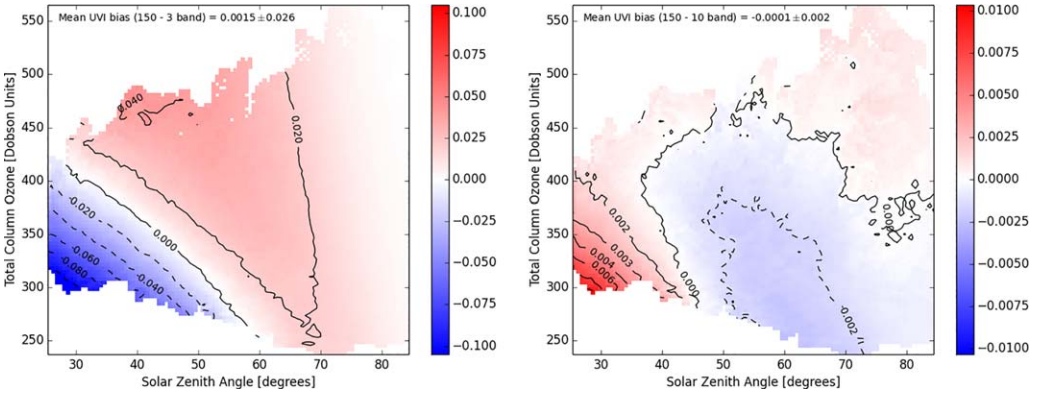

Figure 7. Gridded UK UVI biases between the (left) 3 band and (right) 10 band spectral files and the reference 150 band file shown in Figure 5. All profiles are binned by their total ozone concentration and solar zenith angle and the biases in each bin are the mean. Note the different contour scales.

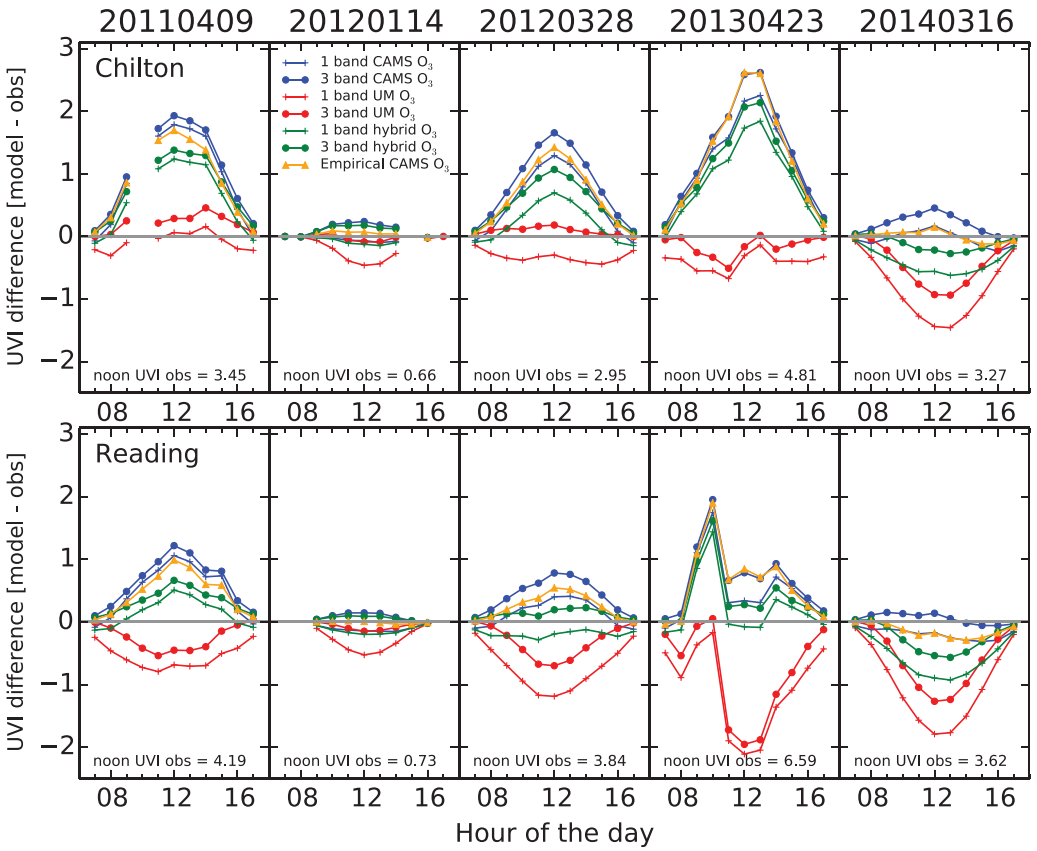

Figure 8. Diurnal UVI biases between fluxes produced by the offline SOCRATES radiation code and observations during low ozone events. (top) For Chilton and (bottom) for Reading. Lines with circles are from the three band spectral file presented in section 3 and lines with crosses are from the original one band file. Blue lines use variable ozone profiles from CAMS, red lines use the monthly climatological ozone from the UM, and green lines use the monthly UM ozone profiles scaled by adding the deviation of the daily CAMS total column ozone from its monthly mean. Orange lines with triangles are from UV indices calculated directly from the empirical model detailed in section 2.3. Breaks in the lines indicate missing observations at that hour.

sites are small in most cases, rarely exceeding 0.5 and only in the April low ozone cases, indicating the two instruments are performing well despite their independent operation. Reading UVI values are always slightly higher than those at Chilton for the days sampled, which is expected due to the slightly lower latitude. Apart from the two days in June where Chilton is higher by about 0.2, which could be due to a number of factors including the higher presence of aerosols, given that Reading is in a semiurban environment, whereas Chilton is rural. There is a clear diurnal pattern to the biases, which is evident in nearly all the days presented, and is primarily a manifestation of a systematic error across the whole day that is constantly proportional to the magnitude of the surface UV at each time, i.e., it peaks at noon. However, the diurnal effect is further enhanced in the one band results because it effectively assumes a constant shape for the solar spectrum across the day, whereas with multiple bands the spectral variation can be more accurately represented. For example, the bias at noon on 15 April 2015 is nearly the same for both band structures in each ozone data set for both sites, yet the diurnal bias is flatter across the day in the three band results, which is the preferable result.

4.1. Low Ozone Events

During a LOE, the total column ozone is far from its climatological value, thus it is expected that incorporating an ozone profile that adequately forecasts the drop would show a large improvement. Figure 8 shows that using variable ozone profiles directly from the CAMS analysis, as opposed to the UM's monthly means, produces increased UVI values by up to 3 during these events. However, the CAMS simulations have a tendency to overshoot the UVI observations whereas those from the existing UM climatology lie closer to, or

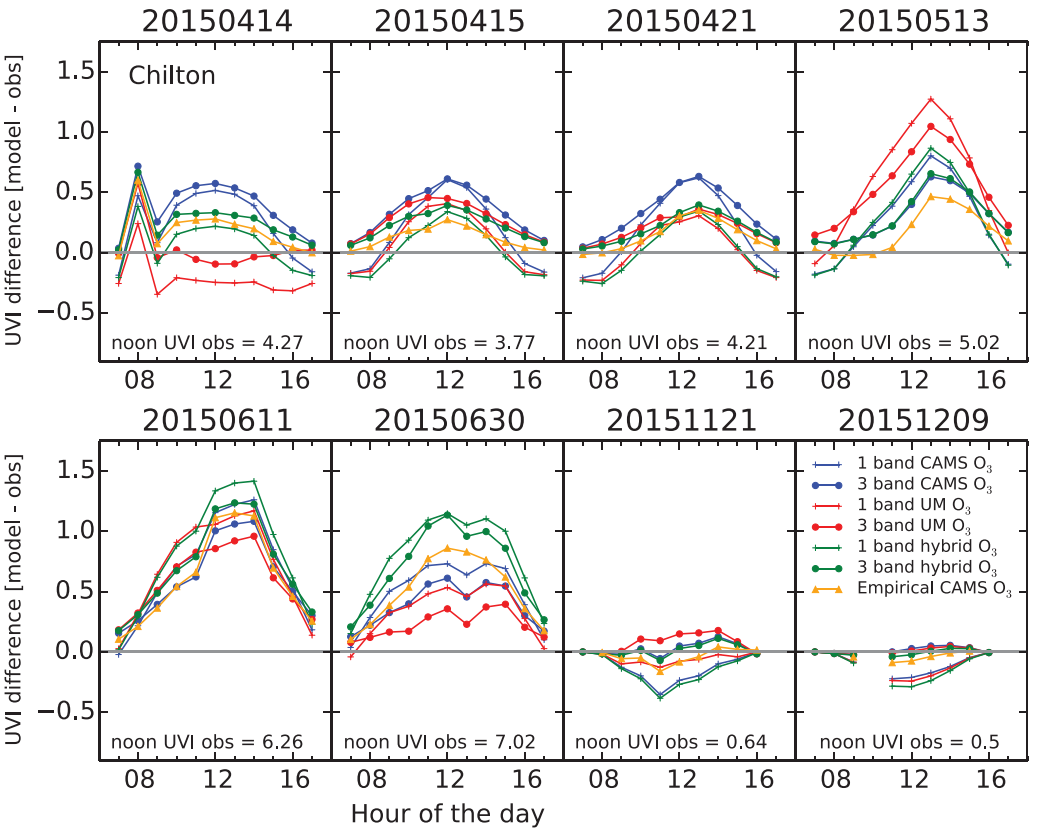

Figure 9. Same as Figure 8 but for a sample of eight clear-sky days with typical ozone levels in 2015 at Chilton. Note the different ordinate scale.

below, the observations. When the UM is scaled by the CAMS variability, errors lie between the original UM and pure CAMS values. A smooth diurnal bias that peaks around noon indicates a constant perturbing factor that is proportional to solar zenith angle such as an incorrect ozone profile for the day, whereas more erratic variations, such as can be seen on 23 April 2013 at Reading, are likely to be due to the presence of cloud contamination. The former suggests that the CAMS product produces too little ozone over the southern UK on the LOE days studied here.

The effect of using a three band rather than a one band spectral file, and hence a more detailed representation of the spectrum, has a less pronounced effect than the choice of ozone profile, with UVI values increasing by up to 0.5 UVI with respect to the one band calculation, indicating the new three band configuration is attenuating less for these low ozone events. When combined with the CAMS ozone the more accurate attenuation coefficients used in the higher resolution spectral file tend to add to the positive bias, because they more accurately represent the lower UV absorption by the underestimated ozone profile. The empirical case that uses the raw CAMS total column ozone performs well for such a simple approximation lying close to the one band CAMS ozone SOCRATES result.

Low ozone biases vary strongly day to day and no single configuration is shown to be consistently better than the others in all cases. For the simulations with variable ozone, this is most likely to be due to the difficulty in forecasting the strength of a low ozone event accurately, coupled with its strong and rapid variation where differences of up to 100 DU can happen within a few hours. As the dominant source of error in these simulations, this in turn makes it difficult to assess the effectiveness of better parameterizing the spectral characteristics which can be better quantified when ozone does not have anomalous values, as follows in the next section.

4.2. Clear-Sky Days

Biases are lower overall on ordinary clear-sky days when ozone is not varying so rapidly and is therefore easier to forecast (Figures 9 and 10). Like for the low ozone cases, the raw CAMS ozone still appears to be an

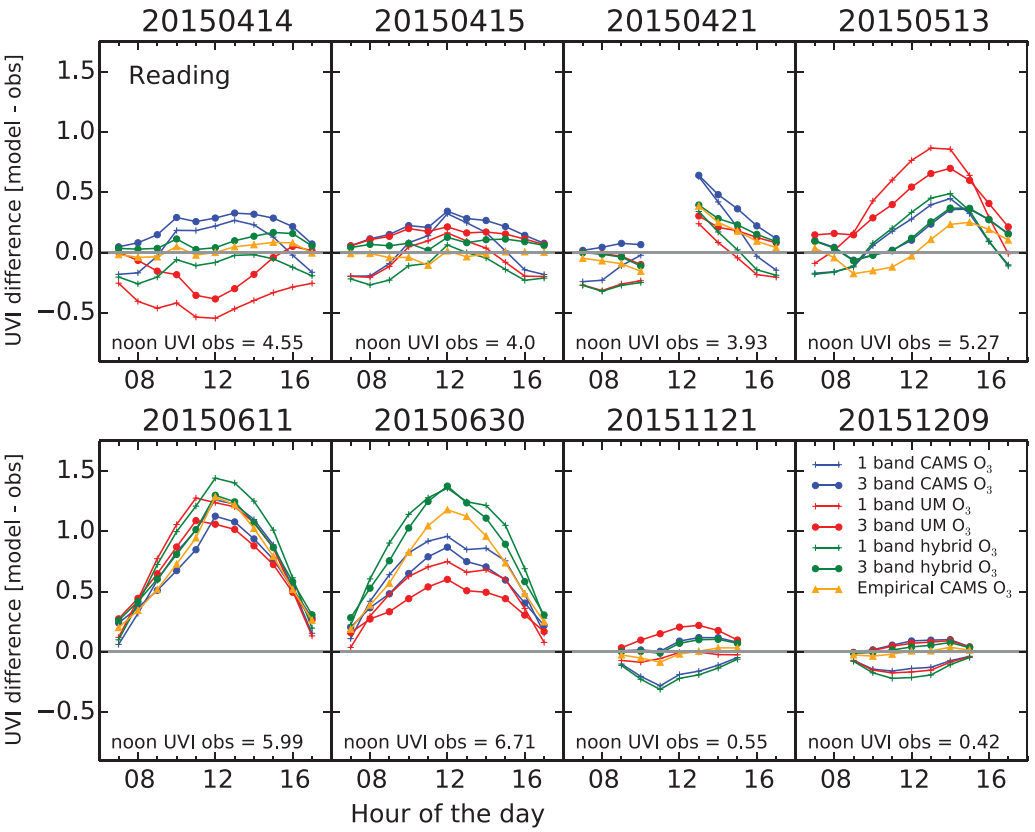

Figure 10. Same as Figure 9 but for Reading.

underestimate with June UVIs are still typically overestimated by around 1 at noon which is 16% of the total measured at that time; however, the three band spectral file reduces biases with respect to the one band file, whether used with the existing UM ozone profile or raw CAMS data, which is a positive result as it is these summer days when accurate UV forecasting is most important. Unfortunately, the hybrid UM product does not improve upon either of the former ozone products indicating errors present in both the mean and the variability (which the original data sets respectively represent) so the hybrid UV product would be a bad choice in these cases. Again the empirical approximation performs surprisingly well across all days sampled, which could indicate that the total column value of CAMS ozone is well estimated, while the vertical profile is not.

4.3. Noontime Biases

Noontime biases are summarized in Figures 11 and 12 as this is the most critical time for sunburn risk. Root-mean-squared errors (RMSEs) over all days in each LOE/clear-sky set for each combination of ozone and spectral configuration are given in Table 1. For low ozone events, the CAMS rescaled UM ozone combined with the existing one band spectral file gives the best mean and RMSE for both sites combined, due to the enhanced representation of the underestimated ozone profile as previously noted. Most of this effect is coming from the Chilton site, if Reading were considered alone the hybrid three band is the configuration with the lowest bias, even more so than the empirical approximation. However, the standard deviation of the one band is larger than the three band for all ozone configurations considered, both low ozone and ordinary clear-sky days, indicating greater variability in performance which might be expected given it is more heavily parameterized.

For 2015 clear-sky days, the mean error for the 1 band hybrid is again lower than the three band hybrid; however, the RMSE is lower in the latter, indicating compensating biases and a much larger spread of values with the one band configuration, as can be seen the error bars in Figure 12. According to Table 1, there is more RMSE consistency between sites for all clear-sky days rather than all low ozone days which is

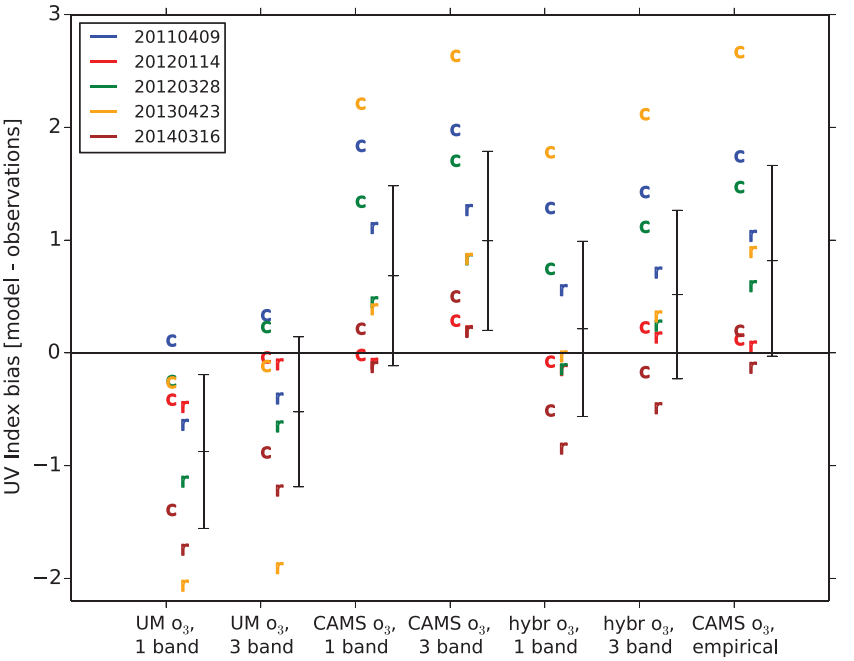

Figure 11. 12:00 UTC UVI biases between UV fluxes, modeled with each of the ozone profile and spectral file combinations labeled on the bottom axis, and observations for low ozone events. "c" markers are for Chilton and "r" are for Reading. Mean and standard deviations are shown to the right of each configuration which includes both sites.

interesting as absolute UV values are at times similar between the two sets of days, and the detectors are supposedly not affected by the total column ozone. It can be seen there is some benefit to using the enhanced 3 band (or 10 band) spectral file in place of the 1 band without changing the climatological ozone profile; however, this does not guard against the effects of increased UV in the event of a sudden drop in ozone, where on average the UVI will be underestimated by 0.5. When including variable ozone it is

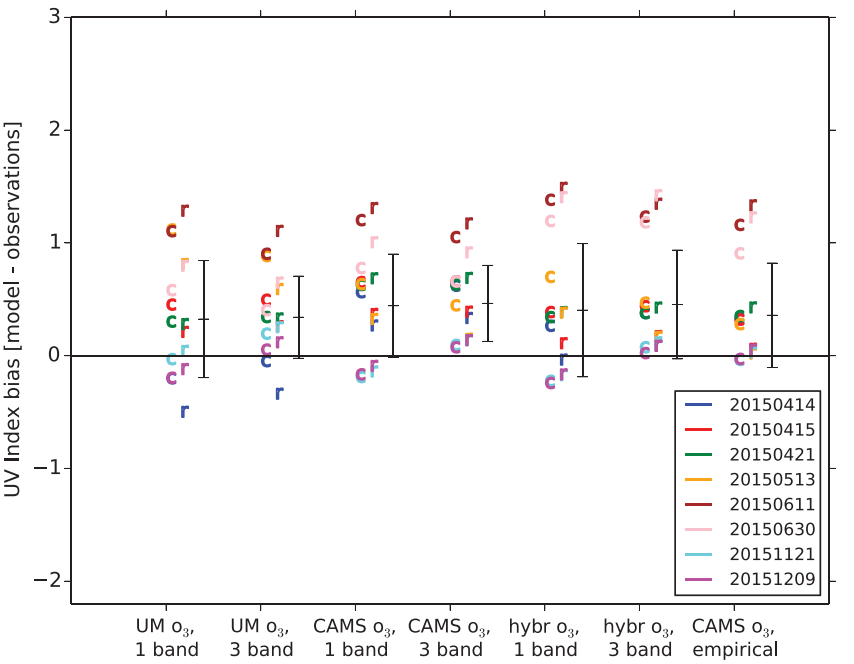

Figure 12. Same as Figure 11 but for 2015 clear-sky days.

Table 1
Root-Mean-Square Error (RMSE) of Noontime Bias Between Modeled Fluxes and Observations for Each Configuration (b = Bands)

Date	UM 1b	UM 3b	CAMS 1b	CAMS 3b	Hybrid 1b	Hybrid 3b	CAMS empir
Low ozone events							
Chilton	0.703	0.450	1.385	1.639	1.034	1.218	1.536
Reading	1.402	1.109	0.539	0.743	0.478	0.413	0.637
Both sites	1.109	0.846	1.051	1.272	0.806	0.909	1.176
2015 clear-sky days							
Chilton	0.603	0.485	0.641	0.569	0.701	0.637	0.536
Reading	0.621	0.512	0.633	0.577	0.729	0.686	0.631
Both sites	0.612	0.499	0.637	0.573	0.715	0.662	0.586

Note. Units are UV Index.

shown that scaling the existing climatology by the CAMS variability, rather than using the raw profile, is preferable, to avoid a substantial overestimation of UVI.

4.4. Spectral Biases

A key advantage of the selected sites is the availability of spectral data, at 1 and 0.5 nm resolution for Chilton and Reading, respectively, allowing the compound UVI bias to be decomposed into its spectral components and so that wavelengths that are contributing most to the error can be identified and possible improvements made. Reading observations are degraded to 1 nm resolution by taking the mean of each pair of fluxes in a 1 nm bin, which corresponds to the trapezoid method of integration. Modeled fluxes in 150 bands sum to total UVI values that are equivalent to the three band values up to the second decimal place.

Figures 13 and 14 show noontime spectral biases as an average of all the days in the low ozone and 2015 clear-sky sets, respectively, for each ozone configuration. The clear-sky biases stay closer to zero but are far more variable from wavelength to wavelength suggesting sources based on the details of the spectrum rather than one that covers a wide spectral band, as is the case with the low ozone set where the greater and more constant errors centered around shorter wavelengths fit the diagnosis of incorrect ozone in the

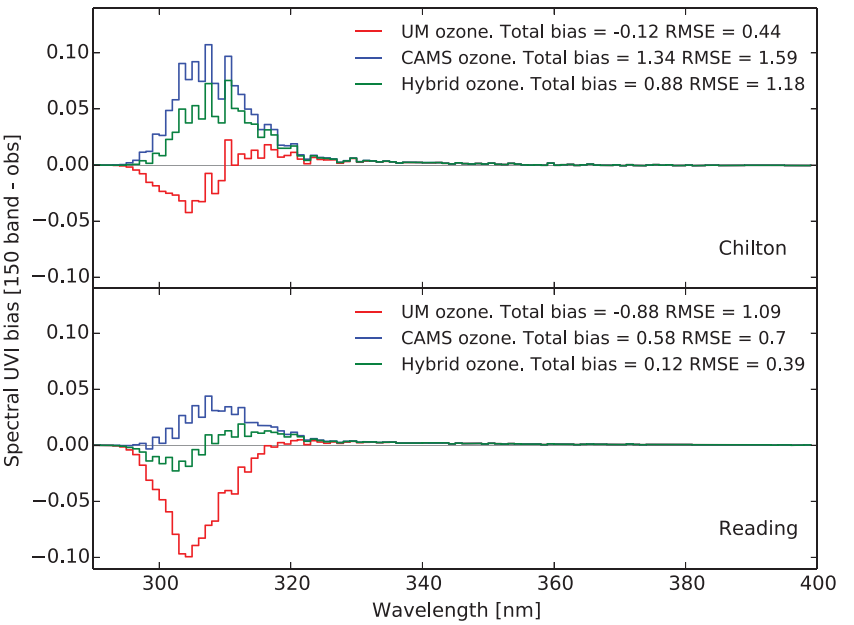

Figure 13. 12:00 UTC spectral UVI biases at 1 nm resolution between modeled UV fluxes (110 bands shown) and observations for low ozone events. Each line is the mean noontime bias of all 5 days for the selected ozone configuration. The total and root-mean-square error over all wavelengths are indicated for each line. Results are split by site, Chilton in the top and Reading in the bottom.

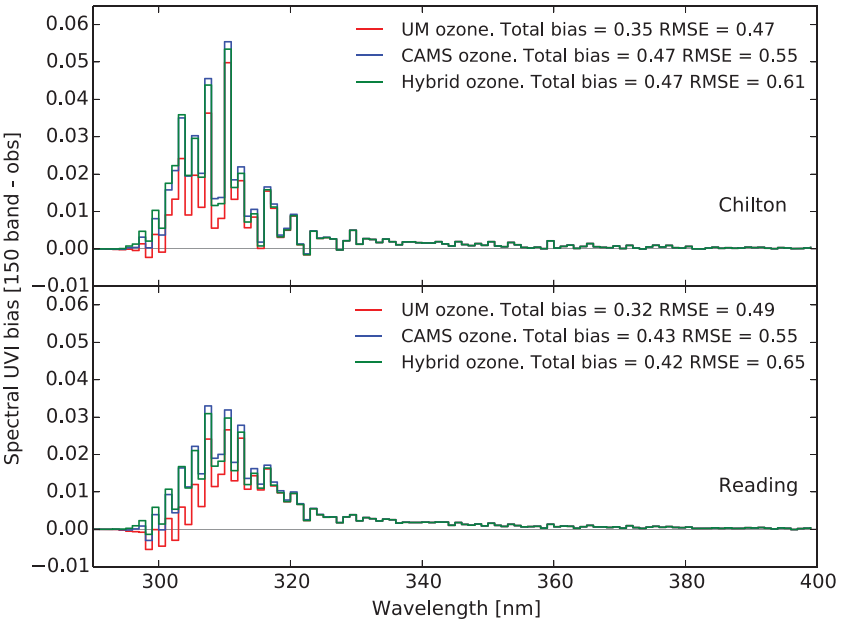

Figure 14. Same as Figure 13 but for 2015 clear-sky days. Each line is the mean noontime bias of all 8 days for the selected ozone configuration.

radiative transfer calculation. In the case of UM ozone at Chilton and hybrid UM-CAMS ozone at Reading, this bias at shorter wavelengths is compensated by a bias of opposite sign at remaining wavelengths to give a very low error in the mean but a larger root-mean-square error (Figure 13). Figure 14 shows that even though Reading and Chilton are very similar in their mean and root-mean-square errors for equivalent ozone configurations (as noted in the previous section), the errors come from different parts of the spectrum which is most likely due to minor differences in the spectral response of the two instruments, e.g., the spike at 310 nm at Chilton which is absent at Reading. These site-to-site differences effectively impose a limit to how accurately the simulated fluxes can be verified in the more common cases where ozone is within expected bounds, suggesting there is limit to the benefits that further improvements in other aspects of the clear-sky simulations can provide.

There is a general lack of extinction modeled across the whole spectrum for typical ozone days and although ozone is the dominant attenuating species at wavelengths up to about 320 nm, aerosols are active across the whole UV band. Further analysis (not shown) of equivalent results produced without applying the erythemal action spectrum to the incoming fluxes reveals biases of equivalent magnitude at longer wavelengths that are masked when the EAS is convolved. Ozone is not active in this region and the biases vary strongly from wavelength to wavelength suggesting a possible lack of aerosols. The aerosols used in the radiative transfer simulations are from the CLASSIC climatology and as such vary month to month but do not reflect local conditions. It is possible that there are more aerosols in the observations which could also contribute to the bias at wavelengths shorter than 320 nm. The strength of the contribution is unknown but it could be significant, for example Krzyścin and Puchalski (1998) found in certain conditions aerosol changes can have an equivalent impact to that of ozone. Modeling the various types of aerosols (there 25 included in the GA7 configuration) in terms of their spectroscopy and atmospheric distribution is not accurately known (Bellouin et al., 2011) and represents an additional source of uncertainty in the simulations. Additionally, absorption of other species not yet modeled at all is also a possibility, such as water vapor which has always been thought to be inactive in the UV region; however, recent studies have suggested it could be responsible for an uncertain amount of extinction (Du et al., 2013; Wilson et al., 2016).

5. Conclusions

An investigation toward improving the UV Index produced by the Met Office operational forecast model is presented. The dual benefits of performing the radiative transfer calculation at a higher spectral resolution

than the existing parameterization (a single band covering 200–320 nm), and ingesting CAMS ozone profiles from ECMWF that vary on a daily basis rather than using the monthly climatology currently implemented within the UM, are assessed and compared. Spectral configurations with 3 and 10 bands between 290 and 400 nm are tuned to within 0.1 UVI of approximate modeled UV indices from a reference 150 band file that covers 250–400 nm, for a year of typical solar zenith angles and ozone profiles experienced by the entire UK.

Diurnal differences between hourly UVI values simulated by offline SOCRATES calculations that use the new spectral configurations and ground-based observations at Chilton and Reading are produced on 13 clear-sky days, 5 of which are identified as low ozone events. It is found that simulations are extremely sensitive to ozone, and that CAMS ozone profiles produce UVI values that are too high across all the days sampled, by up to 3 UVI on a very low ozone day and 1.5 on an ordinary clear-sky day, suggesting the ozone concentration is underestimated over the UK during these events. The current UM climatology based on the SPARC-II data set overestimates ozone for low ozone events as expected but tends to underestimate it for ordinary clear-sky days. A hybrid ozone product based on the current UM climatology, rescaled to include the variable part of the CAMS record, gives better mean results than both former options for the low ozone days, however is not consistently better for typical ozone days. A simple empirical model that uses just total column ozone, solar zenith angle, and Sun-Earth distance as variable inputs performs comparably with the CAMS data and under clear-sky only conditions gives the best RMSE results. However, further progress with this model could only be the result of increased empirical tuning rather than improving the scientific details of the spectrum and furthermore, unlike a radiative transfer calculation, it would be unable to incorporate the effects of clouds or aerosols which is needed if the diagnostic were to be incorporated in an operational forecast model.

The 3, 10, and 150 band spectral configurations give model versus observations biases that are within 0.1 UVI of each other, indicating that the 3 band file would be sufficient to use at the lowest computational cost. Using one of these new configurations as opposed to the former single band parameterization alters UVI by up to 0.5; however, in some cases, this is an increase in bias by representing the already underestimated ozone with more accuracy which overestimates UVI even more. However, all simulations that use a more resolved spectrum show a reduction in the standard deviation of errors over all days sampled, and it is shown that there is some benefit to using the improved spectral file alongside the existing UM ozone climatology. Drilling down further by splitting these biases into their spectral components shows that results that are close to zero in the mean can be due to compensating errors across the spectrum. Comparing results from the two sites on 2015 clear-sky days reveals that even though mean and root-mean-square errors are similar they are made up of biases from different wavelengths. Due to their close proximity and similar modeled fluxes this points toward differences in the instruments' responses at the two sites, and as many of the biases with the hybrid ozone are near zero this suggests limited benefit to improving the spectral representation further.

This study highlights the benefit of including a variable ozone profile in the calculation stage of UV Index but cautions that proper processing is required to ensure the profile itself is consistent with observations. Though raw ingestion of the ozone data set considered in this study would guard against an underestimation of UV Index in the rare case of a low ozone event over the UK, it would overestimate it at all other times. Even when total column values of ozone may be close to observations, as shown by the results of the empirical UV model in this study, it is the vertical distribution of ozone that remains difficult to approximate (Weihs & Webb, 1997), even retrospectively when surface or satellite observations are available (Tegtmeier et al., 2013). Coupled with the uncertainties surrounding the simulation of aerosols it is shown that modeling atmospheric attenuators in the UV region is an ongoing challenge but one that must be achieved before further significant bias reductions are obtained. If this happens the full benefit of a better resolved ultraviolet spectral file can be realized.

Acknowledgments
Thanks to Nina Schuhen and John Penman from the Met Office, Antje Inness and Johannes Flemming from ECMWF, Michael Higlett from PHE, Ann Webb from the University of Manchester and Ben Liley from NIWA for providing data and advice. CAMS data are available from ECMWF at http://apps.ecmwf.int/datasets/data/cams-nrealtime/. The UM data are archived on MASS at moose:/adhoc/users/emma.turner/UV-index-2017, which can be accessed using JASMIN via http://www.ceda.ac.uk/. Data used to generate figures, graphs, plots, and tables are freely available via contacting the lead author: emma.turner@metoffice.gov.uk.

References

Allaart, M., van Weele, M., Fortuin, P., & Kelder, H. (2004). An empirical model to predict the UV-index based on solar zenith angles and total ozone. *Meteorological Applications*, *11*(1), 59–65.

Bellouin, N., Rae, J., Jones, A., Johnson, C., Haywood, J., & Boucher, O. (2011). Aerosol forcing in the climate model intercomparison project (CMIP5) simulations by HadGEM2-ES and the role of ammonium nitrate. *Journal of Geophysical Research*, *116*, D20206. https://doi.org/10.1029/2011JD016074

Bronnimann, S., & Hood, L. L. (2003). Frequency of low-ozone events over northwestern Europe in 1952–1963 and 1990–2000. *Geophysical Research Letters*, *30*(21), 2118. https://doi.org/10.1029/2003GL018431

Brown, A., Milton, S., Cullen, M., Golding, B., Mitchell, J., & Shelly, A. (2012). Unified modeling and prediction of weather and climate: A 25-year journey, *American Meteorological Society*, *93*, 1865–1877. https://doi.org/10.1175/BAMS-D-12-00018.1

Burrows, W. R. (1997). CART regression models for predicting UV radiation at the ground in the presence of cloud and other environmental factors. *Journal of Applied Meteorology*, *36*(5), 531–544.

Carter, O. B., & Donovan, R. J. (2007). Public (mis) understanding of the UV Index. *Journal of Health Communication*, *12*(1), 41–52.

Cionni, I., Eyring, V., Lamarque, J.-F., Randel, W., Stevenson, D., Wu, F., . . . Waugh, D. (2011). Ozone database in support of CMIP5 simulations: Results and corresponding radiative forcing. *Atmospheric Chemistry and Physics*, *11*(21), 11267–11292.

Clark, P., Roberts, N., Lean, H., Ballard, S. P., & Charlton-Perez, C. (2016). Convection-permitting models: A step-change in rainfall forecasting. *Meteorological Applications*, *23*(2), 165–181.

Cusack, S., Edwards, J. M., & Crowther, J. M. (1999). Investigating k distribution methods for parameterizing gaseous absorption in the Hadley Centre Climate Model. *Journal of Geophysical Research*, *104*(D2), 2051–2057. https://doi.org/10.1029/1998JD200063

de Gruij, F. (1995). Action spectrum for photocarcinogenesis. In *Skin cancer: Basic science, clinical research and treatment* (pp. 21–30). Berlin, Germany: Springer.

Du, J., Huang, L., Min, Q., & Zhu, L. (2013). The influence of water vapor absorption in the 290–350 nm region on solar radiance: Laboratory studies and model simulation. *Geophysical Research Letters*, *40*, 4788–4792. https://doi.org/10.1002/grl.50935

Edwards, J., & Slingo, A. (1996). Studies with a flexible new radiation code. I: Choosing a configuration for a large-scale model. *Quarterly Journal of the Royal Meteorological Society*, *122*(531), 689–719.

Flemming, J., Benedetti, A., Inness, A., Engelen, R., Jones, L., Huijnen, V., . . . Katragkou, E. (2016). The CAMS interim reanalysis of carbon monoxide, ozone and aerosol for 2003–2015. *Atmospheric Chemistry and Physics Discussions*, *2016*, 1–82. https://doi.org/10.5194/acp-2016-666

Forster, P. M. d. F. (1995). Modeling ultraviolet radiation at the Earth's surface. Part I: The sensitivity of ultraviolet irradiances to atmospheric changes. *Journal of Applied Meteorology*, *34*(11), 2412–2425.

Gies, P., Roy, C., Javorniczky, J., Henderson, S., Lemus-Deschamps, L., & Driscoll, C. (2004). Global solar UV Index: Australian measurements, forecasts and comparison with the UK. *Photochemistry and Photobiology*, *79*(1), 32–39. https://doi.org/10.1111/j.1751-1097.2004.tb09854.x

Goody, R., West, R., Chen, L., & Crisp, D. (1989). The correlated-k method for radiation calculations in nonhomogeneous atmospheres. *Journal of Quantitative Spectroscopy and Radiative Transfer*, *42*(6), 539–550.

Gorshelev, V., Serdyuchenko, A., Weber, M., Chehade, W., & Burrows, J. P. (2014). High spectral resolution ozone absorption cross-sections—Part 1: Measurements, data analysis and comparison with previous measurements around 293 K. *Atmospheric Measurement Techniques*, *7*, 609–624. https://doi.org/10.5194/amt-7-609-2014

International Standardisation Organisation. (1998). *Erythema reference action spectrum and standard erythema dose* (Rep. ISO 17166/CIE S007/E, Vol. 7, p. E1998).

Jones, A., Roberts, D. L., Woodage, M. J., & Johnson, C. E. (2001). Indirect sulphate aerosol forcing in a climate model with an interactive sulphur cycle. *Journal of Geophysical Research*, *106*(D17), 20293–20310.

Kazantzidis, A., Smedley, A., Kift, R., Rimmer, J., Berry, J. L., Rhodes, L. E., & Webb, A. R. (2015). A modeling approach to determine how much UV radiation is available across the UK and Ireland for health risk and benefit studies. *Photochemical & Photobiological Sciences*, *14*(6), 1073–1081.

Keil, M., Jackson, D., & Hort, M. (2007). The January 2006 low ozone event over the UK. *Atmospheric Chemistry and Physics*, *7*(3), 961–972.

Koepke, P., Bais, A., Balis, D., Buchwitz, M., De Backer, H., de Cabo, X., . . ., Weber, M. (1998). Comparison of models used for UV Index calculations. *Photochemistry and Photobiology*, *67*(6), 657–662.

Krzyścin, J. W., & Puchalski, S. (1998). Aerosol impact on the surface UV radiation from the ground-based measurements taken at Belsk, Poland, 1980–1996. *Journal of Geophysical Research*, *103*(D13), 16175–16181.

Lean, J. L., & DeLand, M. T. (2012). How does the Sun's spectrum vary? *Journal of Climate*, *25*(7), 2555–2560.

Long, C. S., Miller, A. J., Lee, H.-T., Wild, J. D., Przywarty, R. C., & Hufford, D. (1996). Ultraviolet index forecasts issued by the National Weather Service. *Bulletin of the American Meteorological Society*, *77*(4), 729–748.

Manners, J., Thelen, J., Petch, J., Hill, P., & Edwards, J. (2009). Two fast radiative transfer methods to improve the temporal sampling of clouds in numerical weather prediction and climate models. *Quarterly Journal of the Royal Meteorological Society*, *135*(639), Part B, 457–468.

Morcrette, J.-J., & Arola, A. (2007). *A processor to get UV-B and UV-A radiation products in/from the ECMWF IFS*. Reading, UK: European Centre for Medium-Range Weather Forecasts.

Ringer, M., Edwards, J., & Slingo, A. (2003). Simulation of satellite channel radiances in the Met Office Unified Model. *Quarterly Journal of the Royal Meteorological Society*, *129*(589), 1169–1190.

Serdyuchenko, A., Gorshelev, V., Weber, M., Chehade, W., & Burrows, J. P. (2014). High spectral resolution ozone absorption cross-sections—Part 2: Temperature dependence. *Atmospheric Measurement Techniques*, *7*, 625–636. https://doi.org/10.5194/amt-7-625-2014

Setlow, R. B. (1974). The wavelengths in sunlight effective in producing skin cancer: A theoretical analysis. *Proceedings of the National Academy of Sciences of the United States of America*, *71*(9), 3363–3366.

Smedley, A. R., Rimmer, J. S., Moore, D., Toumi, R., & Webb, A. R. (2012). Total ozone and surface UV trends in the United Kingdom: 1979–2008. *International Journal of Climatology*, *32*(3), 338–346.

Tegtmeier, S., Hegglin, M. I., Anderson, J., Bourassa, A., Brohede, S., Degenstein, D., . . . Wang, R. H. J. (2013). SPARC Data Initiative: A comparison of ozone climatologies from international satellite limb sounders. *Journal of Geophysical Research: Atmospheres*, *118*, 12229–12247. https://doi.org/10.1002/2013JD019877

Walters, D., Boutle, I., Brooks, M., Melvin, T., Stratton, R., Vosper, S., . . . Xavier, P. (2017). The Met Office Unified Model Global Atmosphere 6.0/6.1 and JULES Global Land 6.0/6.1 configurations. *Geoscientific Model Development*, *10*(4), 1487–1520.

Webb, A., Aseem, S., Kift, R., Rhodes, L., & Farrar, M. (2016). Target the message: A qualitative study exploring knowledge and cultural attitudes to sunlight and vitamin D in Greater Manchester, UK. *British Journal of Dermatology*, *175*(6), 1401–1403.

Webb, A. R., Kift, R., Berry, J. L., & Rhodes, L. E. (2011). The vitamin D debate: Translating controlled experiments into reality for human sun exposure times. *Photochemistry and Photobiology*, *87*(3), 741–745.

Weihs, P., & Webb, A. R. (1997). Accuracy of spectral UV model calculations: 1. Consideration of uncertainties in input parameters. *Journal of Geophysical Research*, *102*(D1), 1541–1550.

WHO. (2002). *Global solar UV Index: A practical guide: A joint recommendation of the World Health Organization, World Meteorological Organization (WMO), United Nations Environment Programme, and the International Commission on Non-Ionizing Radiation Protection*. Geneva, Switzerland: Author.

Wilson, E. M., Wenger, J. C., & Venables, D. S. (2016). Upper limits for absorption by water vapor in the near-UV. *Journal of Quantitative Spectroscopy and Radiative Transfer*, *170*, 194–199.

Wilson, L. (1993). *Canada's UV Index—How it is computed and disseminated*. Ontario, Canada: Atmospheric Environment Service.

Zhong, W., & Haigh, J. D. (2000). An efficient and accurate correlated-k parameterization of infrared radiative transfer for troposphere–stratosphere–mesosphere GCMs. *Atmospheric Science Letters*, *1*(2), 125–135. https://doi.org/10.1006/asle.2000.0022